Investigation On Structural, Magnetic And Spectral Properties Of CuFe2O4 Nanoparticles

Dr.G.ARUMUGAM[1] Dr.R.KESAVAMOORTHY[2] Dr.A.THIRUVALLUVAR[3]

Assistant Professor of physics PG and Research department of Physics

Annai vailankanni Arts and Science college Thanjavur-7

[3]Principal Govt arts College for women Thanjavur-7

Email id:goviarumugam82@gmail.com

ABSRACT

Cu^{2+} and Fe^{3+} ions mixed ferrite nanoparticles were synthesized by sol-gel auto combustion method XRD pattern confirms the presence of single phase cubic spinel structure from XRD pattern to be 42nm to 43 nm VSM study indicates increased in saturation magnetization and decrease in coercively FE-SEM images exhibit particles with spherical shape and size ranges is found from 37nm to 46nm the two main vibrations of ferrite observed in FT-IR

Keywords

$CuFe_2O_4$ –sol-sel auto combustion method ,structure –magnetic properties

Introduction

Magnetic materials are are used in a varies of application [1.2] magnetic properties like high magnetocrystalline anisotropy large coercively and ideal saturation magnetization.they posses good structural and stability at elevated temperatures substitution of divalent ions like Cu^{2+} and Fe^{3+} of ferrite has been made to vary the structural magnetic and electrical properties (3-6) though several method are available to synthesize ferrites chemical methods are preferred due to their simplicity and chemical homogeneity a fine particle size is required for uniform sintering and

densification which can be obtained easily by chemical methods[7] materials synthesized by sol-gel auto combustion method have high purity chemical homogeneity and uniform particle size ferrite with Cu^{2+} and Fe^{3+} ions was synthesized by sol-gel auto combustion method and their magnetic structural and morphological features were and examined and reported in this work

Experimental Methods

Synthesis of $CuFe_2O_4$ Nanoparticles

Copper ferrite ($CuFe_2O_4$) nanoparticles were synthesized by sol-gel auto combustion method at room temperature. The chemicals used were analytical reagent grade ferric nitrate ($Fe(NO_3)_3.9H_2O$), Copper nitrate ($Cu(NO_3)_2.6H_2O$), citric acid ($C_6H_8O_7.H_2O$) and ammonia (NH_3) solution. Citric acid was employed as the chelating agent. Stoichiometric ratio of nitrates/chelating agent is 1:2. Nitrates and citric acid were dissolved in de-ionized water. This solution was kept in continuous stirring for 24 hrs at 60 °C. The solution become dehydrated and transform into gel. This gel was heat treated in the hot air oven at 250 °C for 8 hrs. This leads to the formation of a dark loose powder. The powder was heated at a rate of 5 °C/min in a muffle furnace and kept at 800 °C for 4 hrs. Finally it was grained finely using mortar and pestle for further analysis. The following instruments were used to synthesis of $NiFe_2O_4$ nanoparticles.

RESULTS AND DISCUSSION

6.1 Powder X-ray diffraction (XRD) analysis

Structural and phase analysis of copper ferrite nanoparticles were investigated by powder XRD patterns (X'Pert-PRO Pan Analytical X-ray diffractometer operated at 45 kV and 30 mA, Cu Kα, wavelength 1.5406 Å). The diffracted pattern of synthesized copper ferrite is shown in Fig. 23. The diffracted XRD pattern confirms the presence of a single phase cubic spinel structure. The prominent hkl planes (220), (311), (222), (400), (422), (511) and (440) are identified and indexed. The results are in good agreement with JCPDS Card NO.: 77-0010 [44-46].

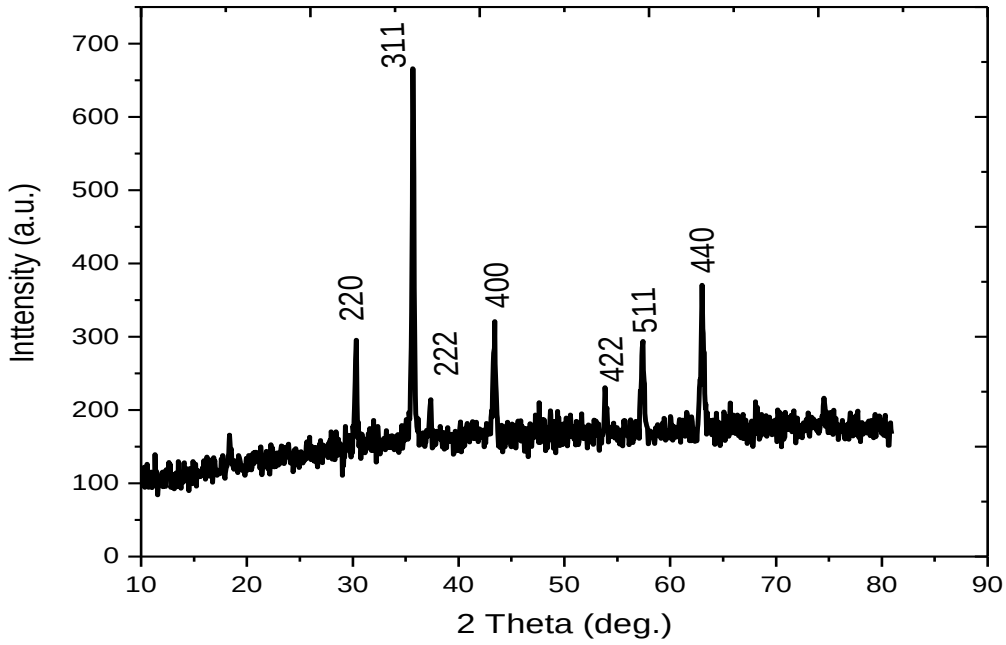

Fig. 23: XRD pattern of $CuFe_2O_4$ nanoparticles

The lattice parameters were calculated using the formula,

$$d = \frac{a}{\sqrt{h^2 + k^2 + l^2}}$$

where, "d" is inter-planar distance, "h, k and l" are the miller indices [47]. The determined lattice constant values are given in Table 1. With the help of Scherer equation,

$$D = \frac{0.9\lambda}{\beta \cos\theta}$$

The average crystallite size (D) was calculated. Here, λ is wavelength of the X-ray radiation used, β is full width at half maximum (FWHM) measured in radians and θ is Bragg angle. The

crystallite sizes were found to vary from 42 nm. The X-ray density (ρ_x) of copper ferrite nanoparticles were calculated using,

$$\rho_x = \frac{8M}{Na^3}$$

where, 8 denotes the number of atoms in a unit cell of spinel lattice, M is molecular mass of the particular ferrite nanoparticles, N is the Avogadro's number (6.02252×10^{26} $kmol^{-1}$) and 'a' is the lattice constant. The calculated values of X-ray density is 5.415 g/cm^3 for copper ferrite nanoparticles.

Table 1: Structural and magnetic properties of copper ferrite nanoparticles

Properties		**$CuFe_2O_4$ ferrite**
Lattice constant (a) (Å)		8.346
Volume (V) ($Å^3$)		581.34
Crystallite size (nm)	XRD data	42.43
	FE-SEM image	37-46
X-ray density (g/cm^3)		5.415
Saturation magnetization (Ms) (emu/g)		25.37
Coercivity (Hc) (Oe)		198

Remanence magnetization (Mr) (emu/g)	7.6
Bohr magneton (μ_B)	1.06

6.2 Vibrating Sample Magnetometer (VSM) analysis

Magnetization measurements of $CuFe_2O_4$ samples were done using vibrating sample magnetometer (VSM-Lake Shore model 7404, operated at a maximum applied field of 12.5 kOe at room temperature). The observed hysteresis (M-H) curves are presented in Fig. 24 and 25. From the plotted M-H curves, the saturation magnetization (Ms), coercivity (Hc) and remanent magnetization (Mr) values are measured.

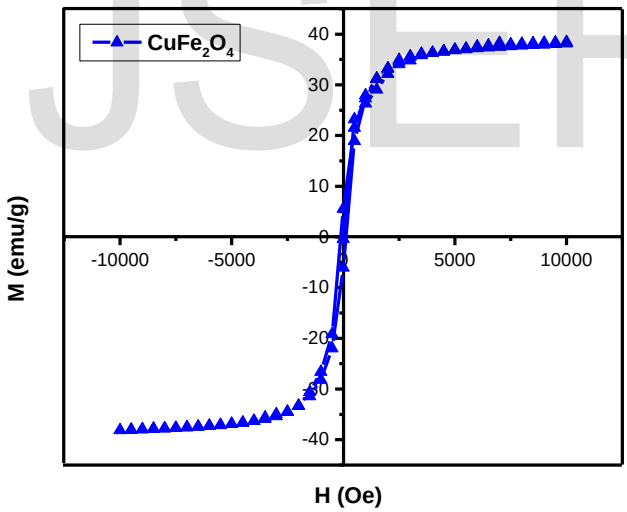

Fig. 24: M-H plots of $CuFe_2O_4$ nanoparticles

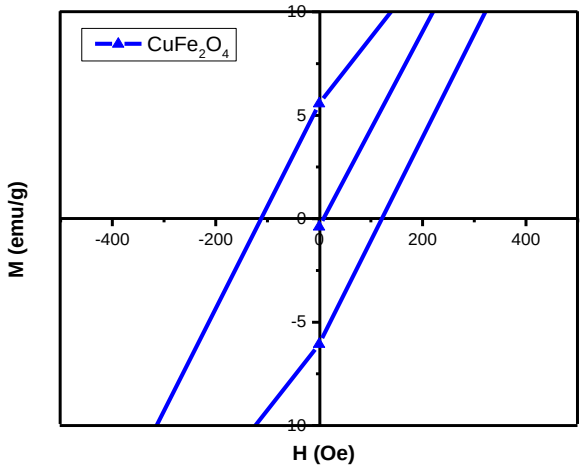

Fig. 25: M-H enlarged plot of $CuFe_2O_4$ nanoparticles

The experimental magnetic moment per formula unit in Bohr magneton (μ_B) was calculated from the saturation magnetization values using the equation,

$$\mu_B = \frac{M_S M_W}{5585}$$

where, M_S is saturation magnetization, M_W is molecular weight of the $CuFe_2O_4$ sample and 5585 is magnetic factor. The observed values are listed in Table 1. The M-H curves revealed that the magnetic properties of the nanoparticles are affected by composition and different cation distribution. Various cations can be occupied in tetrahedral sites and octahedral sites to change the magnetic properties [48]. All the hysteresis curves indicate soft ferromagnetic nature of the nanoparticles. The saturation magnetization value of $CuFe_2O_4$ ferrite sample is 25.37 emu/g with maximum applied field 12.5 kOe at room temperature. Which is agree with results reported by Mahmoud Goodarz et al [49].

6.3 Field Emission Scanning Electron Microscopy (FE-SEM) analysis

The morphological features of $CuFe_2O_4$ ferrite samples were analyzed by FE-SEM analysis (Model-JEOL/JSM-5610 NE instrument) and are shown in Fig. 26. The grain size of the heat treated samples is found to be from 37 nm to 46 nm for nickel ferrite. FE-SEM images

revealed the spherical nature of the particles. Observed particle size closely matches with the values obtained from XRD measurement.

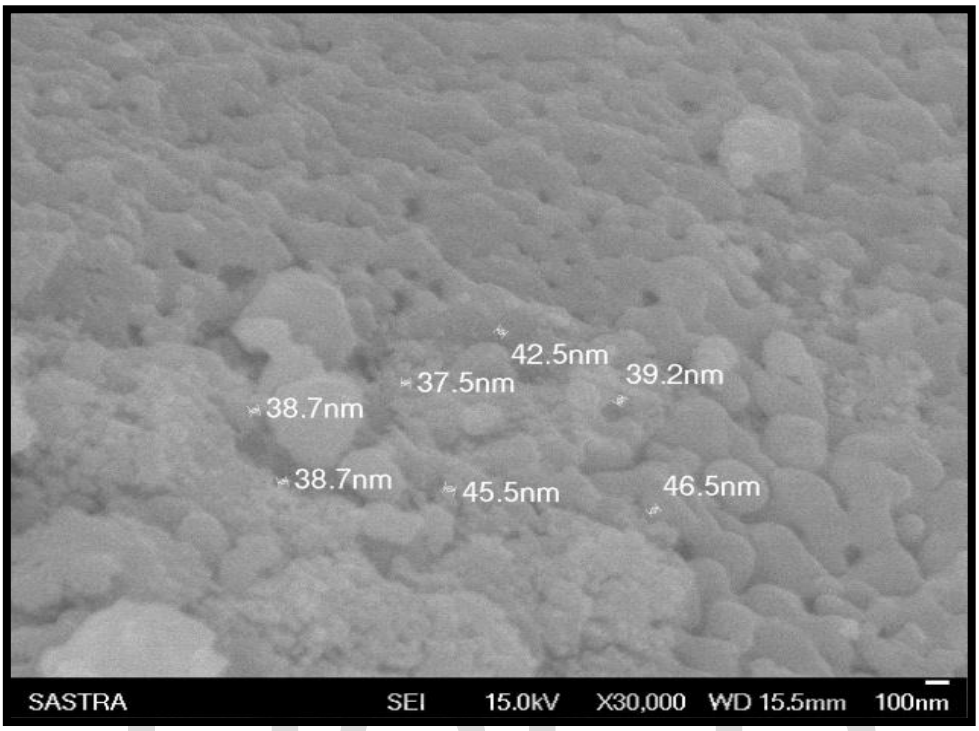

Fig. 26: FE-SEM image of $CuFe_2O_4$ nanoparticles

6.4 FT-IR spectral study

FT-IR spectra of $CuFe_2O_4$ ferrite samples were recorded using Perkin Elmer FT-IR spectrometer in the range 4000 to 400 cm^{-1} and are shown in Fig. 27. The unit cell of nickel ferrite contains 8 molecules. There are 32 divalent oxygen ions, 16 trivalent iron ions and 8 divalent nickel ions in the unit cell. 32 oxygen atoms arrange themselves in fcc structure and this leads to 8 tetrahedral voids (A-sites) and 16 octahedral voids (B-sites). The copper ions occupy half of the B-sites. The remaining B-sites and A-sites are occupied by iron ions. Ni^{2+} ion is expected to occupy B-sites. This divalent metal ion may also occupy A-sites and B-sites which results in the movement of iron ions from A-sites to B-sites [50].

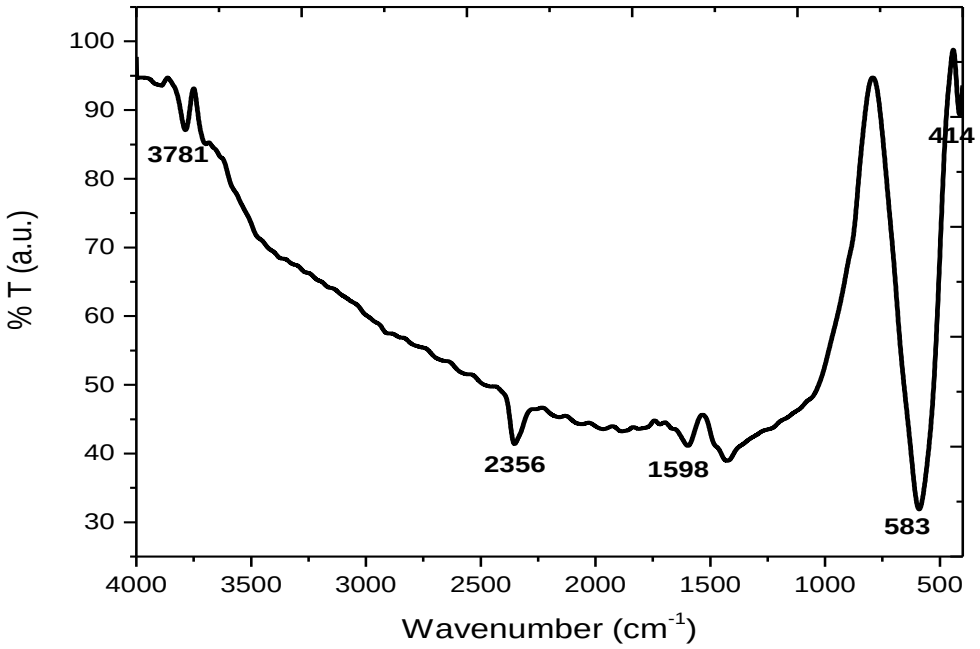

Fig. 27: FT-IR spectrum of $CuFe_2O_4$ nanoparticles

The two main vibrations of tetrahedral and octahedral metal-oxygen bonds will be observed in the range of 800-400 cm^{-1}. The band observed around 583 cm^{-1} - 598 cm^{-1} and 414 cm^{-1} - 421 cm^{-1} is due to tetrahedral sites and octahedral sites respectively. In $CuFe_2O_4$, the tetrahedral M-O vibration occurs at 583 cm^{-1} and the octahedral M-O vibration of $CuFe_2O_4$ occurs at 414 cm^{-1}. The occurrence of two metal-oxygen (M-O) vibrations at two different wavenumbers is due to the change in metal-oxygen bond length for tetrahedral and octahedral sites. The observed absorption bands closely match with earlier literature values [51, 52].

6.5 Energy Dispersive X-ray (EDAX) analysis

The chemical composition of nanoparticles was estimated by EDAX technique. The EDAX pattern confirms homogeneous mixing of Cu, Fe, and O atoms in room temperature and annealed nanoparticles. The detailed estimated composition of $CuFe_2O_4$ ferrite nanoparticles is shown in Table 2. The observed composition is almost equal to that of the nanoparticles produced by stoichiometric calculations while taking oxygen as balanced. The stoichiometric of the

compositions of the prepared spinel was checked by EDAX analysis and the results obtained are given in Fig. 28 (a) and (b). It has been found that there is a good agreement between the experimentally obtained atom percentage of the elements and the theoretically calculated atom percentage. We have observed no other peaks except the extra gold (Au) peak. The gold peak appears due to the thin coating on the nanoparticles surface to make it conducting, which is required to record the FE-SEM picture. It reveals that there is no contamination in the nanoparticles. The metal content stoichiometric of the compounds used for the preparation of the nanoparticles was taken as theoretical composition while the observed stoichiometric was calculated from EDAX studies.

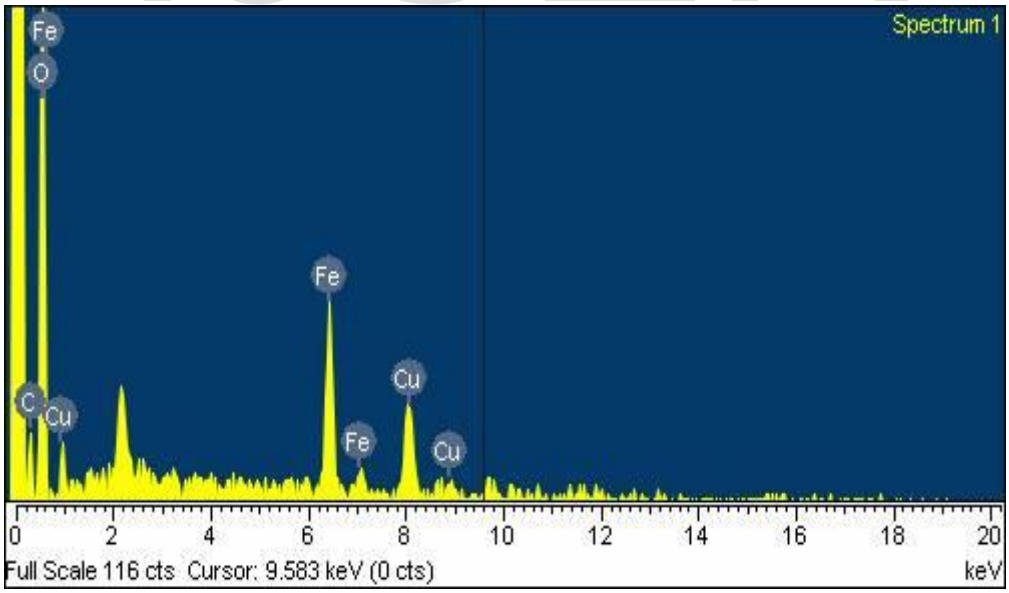

Fig. 28 (a): EDAX spectrum of as synthesized $CuFe_2O_4$ nanoparticles

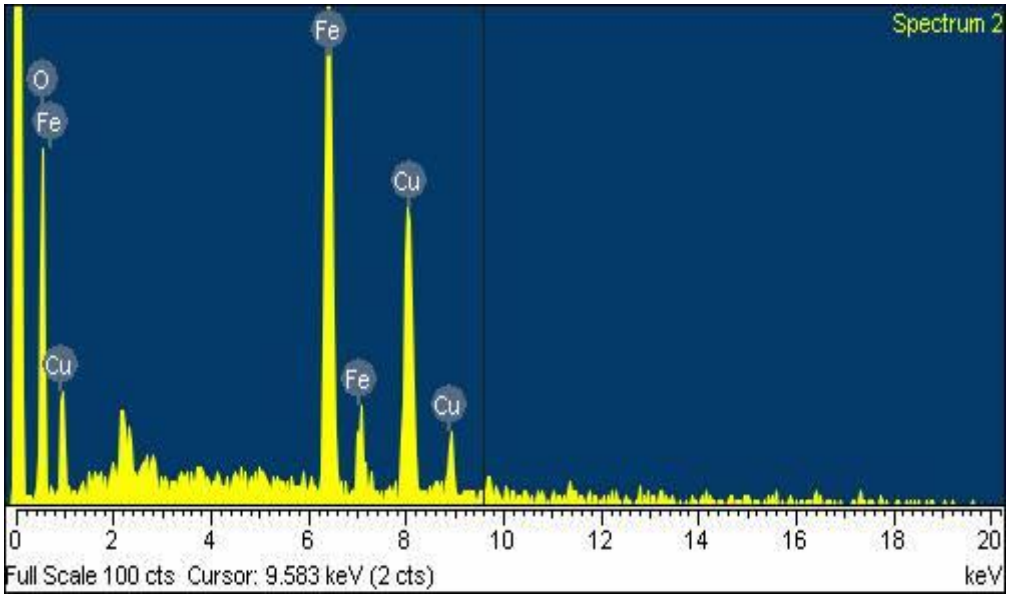

Fig. 28 (b): EDAX spectrum of annealed $CuFe_2O_4$ nanoparticles

Table 2: The elemental composition of $CuFe_2O_4$ nanoparticles

Element	Intensity	Weight %	Atomic %
O K	1.2697	0.40	46.88
Fe K	1.0305	0.76	25.47
Cu K	0.8913	0.93	27.65

The stoichiometric of the powder nanoparticles in the methods was checked by EDX analysis. Sol–gel derived the nanoparticles shows expected stoichiometric nickel deficiency and the presence of excess oxygen. Sol-Gel yields $CuFe_2O_4$ particles of very small size and hence specific surface area of the particles becomes very large. So the possibility of oxygen adsorption is high and this may be the reason for excess oxygen. No trace of any impurity was found which indicates purity of the nanoparticles.

7. CONCLUSION

Copper ($CuFe_2O_4$) ferrite nanoparticles were synthesized at room temperature by sol-gel auto combustion method. The synthesized nanoparticles were crystallized in cubic spinel phase with Fd3m space group. The lattice parameter and average crystallite size values are calculated from XRD pattern. The magnetic properties such as saturation magnetization (M_s), coercivity (H_c) and remanent magnetization (M_r) values are calculated from M-H plotted loop. FE-SEM image revealed that the synthesized $CuFe_2O_4$ nanoparticles are spherical in shaped and size of the particles was found to from 37 nm to 46 nm, which is confirmed by the XRD pattern. The presences of two main metal (M-O) ion vibrations of tetrahedral (A) sites at 583 cm^{-1} and octahedral (B) sites at 411 cm^{-1} were observed in FT-IR spectra. The presence of Cu, Fe and

Oxygen ions are confirmed by the EDAX spectrum and their estimated theoretical values are calculated from the EDAX spectrum. From the all the characterizations revealed that the Cu ferrite nanoparticles possess the good structural, surface morphological and magnetic properties. So that, the Cu ferrite nanoparticles is opted for fabrication of magnetic data storage devices.

Acknowledgments

Author.Dr.G.ARUMUGAM VSM Characterization facilities Alagappa University karaikudi for powder XRD facilities St Jesoph's College ,Tiruchirappalli for FT-IR spectra and SASTRA University thanjavur for FE-SEM facilities.

REFERENCES

[1] Charles Kittle, Introduction to Solid State Physics, 5th edition, John wiley & sons, New York (1976).

[2] S. Chickazumi, S.H. Charap, Physics of Magnetism, Krieger Malabar (1978).

[3] Nicola A. Spaldin, Magnetic materials fundamental and applications, Cambridge University, Cambridge, UK (2011).

[4] B.S. Murthy, P. Shankar, Balder Raj, B.B. Rath, James Murday, A text book of Nanoscience and nanotechnology, Springer-verlag Berlin Heidelberg Edition num-1, (2013).

[5] K.H.J. Buschow, A Hand book of magnetic materials, Elsevier- North Holland, 1 (1998).

[6] Q. Chen, Z.J. Zhang, Size-dependent superparamagnetic properties of $MgFe_2O_4$ spinel ferrite nanocrystalline, J. Appl. Phys. Lett. 73 (1998) 3156–3158.

[7] Z.X. Tang, C.M. Sorensen, K.J. Klabunde, G.C. Hadjipanayis, Preparation of Mn ferrite fine particles from aqueous solution, J. Colloid Interface Sci. 146 (1991) 38–46.

[8] C.T. Seip, E.E. Carpenter, C.J. O Connor, V.T. John, S. Li, Magnetic properties of a series of ferrite nanoparticles synthesized in reverse micelles, IEEE Trans. Magn. 34 (1998) 1111–1113.

[9] J.F. Hochepied, P. Bonville, M.P. Pileni, Non stoichiometric zinc ferrite nanocrystals: syntheses and unusual magnetic properties, J. Phys. Chem. B 104 (2000) 905–912.

[10] C. Liu, B. Zou, A.J. Rondinone, Z.J. Zhang, Reverse micelle synthesis and characterization of superparamagnetic $MnFe_2O$ spinel ferrite nano crystallites, J. Phys. Chem. B 104 (2000) 1141–1145.

[11] V.G. Bashtovoy, B.M. Berkovsky, A.N. Vislovich, Introduction to magnetic fluids. Washington (1988).

[12] N.A. Brusentsov, L.V. Nikitin, T.N. Brusentsova, A.A. Kuznetsov, F.S. Bayburtskiy, L.I. Shumakov, N.Y. Jurchenko Magnetic fluid hyperthermia of the mouse experimental tumor, J. Magn. Magn. Mater., 252 (2002) 378.

[13] Richard M. Bozorth, Ferromagnetism, first published 1951, reprinted 1993 by IEEE Press, New York.

[14] W. Andra, U. Hafeli, R. Hergt and R. Misri, Applications of magnetic particles ion medicine and biology, Handbook of Magnetism and Advanced Magnetic Materials, John Wiley & Sons. (2007) 2536-2568.

[15] J.M.D. Coey, Magnetism and Magnetic Materials, Cambridge University Press, USA (2010) 555-565.

[16] C.W. Nan, M.I. Bichurin, S. Dong, D. Viehland and G. Srinivasan, Multiferroic magnetoelectric composites: Historical perspective, status, and future direction, J. Appl. Phys. 103 (2008) 1-35.

[17] W. Eerenstein, N.D. Mathur and J.F. Scott, Multiferroic and magnetoelectric materials, Nature, 442 (2006) 759-765.

[18] C.N.R. Rao, C.R. Serraoab, New routes to multiferroics, J. Mater. Chem. 17 (2007) 4931–4938.

[19] R. Liu, Y. Zhao, R. Huang, Y. Zhao, and H. Zhou, Multiferroic ferrite/perovskite oxide core/shell nanostructures , J. Mater. Chem. 20 (2010) 10665-10670.

[20] K. Raydongia, A. Nag, A. Sundaresan, and C.N.R. Rao, Multiferroic and magnetoelectric properties of core-shell $CoFe_2O_4$@$BaTiO_3$ nano composites, Appl. Phys. Lett. 97 (2010) 1-3.

[21] A.R. West, Solid State Chemistry and its Applications, John Wiley and Sons (1984).

[22] J. Smit, H.P.J. Wijn Ferrites (Philips Technical Library, Eindhoven, 1959.

[23] Robert C. Pullar, Hexagonal ferrites: A review of the synthesis, properties and applications of hexaferrite ceramics, Progress in Materials Science 57 (2012) 1191–1334.

[24] X. Obradors, A. Collomb, M. Pernet, X-Ray Analysis of the Structural and Dynamic Properties of $BaFe_{12}O_{19}$ Hexagonal Ferrite at Room Temperature, J. Solid State Chemistry, 56 (1985) 171-181.

[25] Yue Liu, Michael G.B. Drew, Ying Liu, Preparation and magnetic properties of barium ferrites substituted with manganese, cobalt, and tin, J. Magn. Magn. Mate. 323 (2011) 945–953.

[26] Sinan Dursun, Ramazan Topkaya, Numan Akdogan, Sedat Alkoy, Comparison of the structural and magnetic properties of submicron barium hexaferrite powders prepared by molten salt and solid state calcinations routes, Ceramics International 38 (2012) 3801–3806.

[27] Suriya Ounnunkad, Improving magnetic properties of barium hexaferrites by La or Pr substitution, Solid State Communications 138 (2006) 472–475.

[28] J. Jiang, L.H. Ai, $SrFe_{12}O_{19}$/ZnO hybrid structures: Synthesis, characterization and properties, J. Alloys and Compds. 502 (2010) 488–490.

[29] F. Khademi, A. Poorbafrani, P. Kameli, H. Salamati, Structural, Magnetic and Microwave Properties of Eu-doped Barium Hexaferrite Powders, J. Supercond. Nov. Magn. 25 (2012) 525–531.

[30] J. Kreisel, H. Vincent, F. Tasset, M. PateH, J.P. Ganne, An investigation of the magnetic anisotropy change in $BaFe_{12-2x}Ti_xCo_xO_{19}$ single crystals, J. Magn. Magn. Mater. 224 (2001) 17-29.

[31] Seema Joshi, Manoj Kumar,Influence of Co^{2+} Substitution on Cation Distribution and on Different Properties of $NiFe_2O_4$ Nanoparticles. J. Supercond Novel Magn. 29 (6), 1561-1572 (2016)

[32] Balavijayalakshmi, J. Suriyanarayanan, N., Jayaprakash, R.: Role of copper on structural, magnetic and electric properties of nickel ferrite nano particles. J. Magn. Magn. Mater. 385, 302-307 (2015)

[33] Xiaoyan Tan, Guiying Li, Ying Zhao, Changwei Hu.: Effect of preparation method on the surface properties and activity of $Ni_{0.7}Cu_{0.3}Fe_2O_4$ nanoparticles. J. Alloys Compd. 493, 55-63 (2010)

[34] Mahmoud Goodarz Naseri, Elias Saion, Nasrin Khalil Zadeh, The amazing effects and role of PVP on the crystallinity, phase composition and morphology of nickel ferrite nanoparticles prepared by thermal treatment method, Int. Nano Let. 3 (19) 2013 1-8

[35] Khalid Mujasam Batoo, M.S. Abd El-sadek. Electrical and magnetic transport properties of Ni-Cu-Mg ferrite nanoparticles prepared by sol-gel method. J. Alloys Compd. 566, 112-119 (2013)

[36] Xiangyuan Liu, John Wang, Leong-Ming Gan, Sen-Choon Ng, Jun Ding, An ultrafine barium ferrite powder of high coercivity from water-in-oil microemulsion, J. Magn. Magn. Mate. 184 (1998) 344-354.

[37] K.S. Martirosyana, E. Galstyan, S.M. Hossain, Yi-Ju Wang, D. Litvinov, Barium hexaferrite nanoparticles: Synthesis and magnetic properties, Materials Science and Engineering B 176 (2011) 8–13.

[38] Q. Mohsen, Barium hexaferrite synthesis by oxalate precursor route, J. Alloys and Compds. 500 (2010) 125–128.

[39] Jianxun Qiu, Mingyuan Gu, Crystal structure and magnetic properties of barium ferrite synthesized using GSPC and HEBM, J. Alloys and Compds. 415 (2006) 209–212.

[40] S. Bierlich, T. Reimanna, H. Bartsch, J. Töpfer, Co/Ti-substituted M-type hexagonal ferrites for high-frequency multilayer inductors, J. Magn. Magn. Mater. 384 (2015) 1–5.

[41] Sonal Singhal, Tsering Namgyal, Jagdish Singh, Kailash Chandra, Sandeep Bansal, A comparative study on the magnetic properties of $MFe_{12}O_{19}$ and $MAlFe_{11}O_{19}$ (M = Sr, Ba and Pb) hexaferrites with different morphologies, Ceramics International 37 (2011) 1833–1837.

[42] Yujie Yang, Xiansong Liu, Dali Jin, Yuqi Ma, Structural and magnetic properties of La–Co substituted Sr–Ca hexaferrites synthesized by the solid state reaction method, Materials Research Bulletin, 59 (2014) 37-41.

[43] J. Matutes Aquino, S. Diaz Castanon, M. Mirabal Garciac, S.A. Palomares Sanchez, Synthesis by co-precipitation and study of Barium Hexaferrite powders, J. Scripta mater. 42 (2000) 295–299.

[44] Roberto Köferstein, Till Walther, Dietrich Hesse, Stefan Ebbinghaus, G.: Crystallite-growth, phase transition, magnetic properties and sintering behavior of nano-$CuFe_2O_4$ powders prepared by a combustion-like process. J. Solid State Chem. 213 (2014) 57-64.

[45] Zhipeng Sun, Lang Liu, Dian zeng Jia, Weiyu Pan.: Simple synthesis of $CuFe_2O_4$ nanoparticles as gas-sensing materials. J. Sensors & Actuators B 125 (2007) 144-148.

[46] Gopathi Ravi Kumar, Katrapally Vijaya Kumar, Yarram Chetty Venudhar.: Synthesis, Structural and Magnetic Properties of Copper Substituted Nickel Ferrites by Sol-Gel Method. J. Mattr. Sci. & Appl. 3 (2012) 87-91.

[47] R. Kesavamoorthi, C. Ramachandra Raja, Structural and Magnetic Properties of Cobalt and Copper Ions Mixed Nickel Ferrite Nanoparticles, J. Supercond. Nov. Magn. 30 (2017) 2535–2540.

[48] Balavijayalakshmi, J., Suriyanarayanan, N., Jayaprakash, R.: Role of copper on structural, magnetic and electric properties of nickel ferrite nano particles. J. Magn. Magn. Mater. 385 (2015) 302-307.

[49] Patil, D.R., Chougule, B.K.: Effect of copper substitution on electric and magnetic properties of $NiFe_2O_4$ ferrite. J. Mater. Chem. Phys. 117 (2009) 35-40.

[50] Minoo Ghaani, Jilla Saffari.: Synthesis of $CuFe_2O_4$ Nanoparticles by a new co-precipitation method and using them as Efficient Catalyst for One-pot Synthesis of Naphthoxazinones. J. Nanostruct., 6 (2) (2016) 172-178.

[51] Kargar, Z., Asgarian, S.M., Mozaffari, M.: Positron annihiliation and magnetic properties of copper substituted nickel ferrite nanoparticles. J. Nuclear Instr. Methods in Phys. Res. B. 375 (2016) 71-78.

[52] Saima Sultana, Rafiuddin, Mohammad Zain Khan, Khalid Umar, Synthesis and characterization of copper ferrite nanoparticles doped polyaniline, J. Alloys and Compds. 535 (15) (2012) 44-49.